

# Spin polaron theory for the photoemission spectra of layered cobaltates

Jiří Chaloupka<sup>1,2</sup> and Giniyat Khaliullin<sup>1</sup>

<sup>1</sup>*Max-Planck-Institut für Festkörperforschung, Heisenbergstrasse 1, D-70569 Stuttgart, Germany*

<sup>2</sup>*Department of Condensed Matter Physics, Faculty of Science,  
Masaryk University, Kotlářská 2, 61137 Brno, Czech Republic*

(Dated: January 3, 2022)

Recently, strong reduction of the quasiparticle peaks and pronounced incoherent structures have been observed in the photoemission spectra of layered cobaltates. Surprisingly, these many-body effects are found to increase near the band insulator regime. We explain these unexpected observations in terms of a novel spin-polaron model for  $\text{CoO}_2$  planes which is based on a fact of the spin-state quasidegeneracy of  $\text{Co}^{3+}$  ions in oxides. Scattering of the photoholes on spin-state fluctuations suppresses their coherent motion. The observed “peak-dip-hump” type lineshapes are well reproduced by the theory.

PACS numbers: 71.27.+a, 79.60.-i, 72.10.Di

Strongly correlated behavior of electrons is a common property of transition metal oxides. This is because the bandwidth in these compounds is relatively small compared to the intraionic Coulomb repulsion between the  $3d$  electrons. As a result, the celebrated Mott physics [1] forms a basis for understanding of a unique properties of oxides, such as the high- $T_c$  superconductivity and a colossal magnetoresistivity.

Recently, attention has focused on the layered cobalt oxides because they exhibit high thermoelectric power [2], i.e., the capability to transform heat energy into electricity. These compounds consist of a triangular lattice  $\text{CoO}_2$  planes, separated either by Na layers like in  $\text{NaCoO}_2$  [3] or by thick layers of rock-salt structure in so-called “misfit” cobaltates (see [4, 5] and references therein). Besides controlling the  $c$ -axis transport, the Na and rock-salt layers introduce also the charge carriers into the  $\text{CoO}_2$  planes, such that the valence state of Co ions is varied in a wide range from nonmagnetic  $\text{Co}^{3+t_{2g}^6}$   $S = 0$  state (as in  $\text{NaCoO}_2$ ) towards the magnetic  $\text{Co}^{4+t_{2g}^5}$   $S = 1/2$  configuration (in  $\text{Na}_x\text{CoO}_2$  at small  $x$ ).

As the  $t_{2g}^6$  shell of  $\text{Co}^{3+}$  is full, this limit is naturally referred to as a band insulator [6, 7], while  $\text{Co}^{4+}$   $S = 1/2$  rich compounds fall into the category of Mott systems because of unquenched spins. It has therefore been thought that layered cobaltates may provide an interesting opportunity to monitor the evolution of electronic states from a weakly correlated band-insulator regime to the strongly correlated Mott-limit by hole doping of  $\text{NaCoO}_2$ . Surprisingly, a completely opposite trend is found experimentally. The hallmarks of strong correlations such as magnetic order [3, 8], strong magnetic field effects [2], *etc.*, are most pronounced closer to the  $\text{Co}^{3+}$  compositions, while  $\text{Co}^{4+}$   $S = 1/2$  rich compounds behave as a moderately correlated metals [3, 9]. The best thermoelectric performance of cobaltates is also realized near the doped band insulator regime [10], thus unusual correlations in this state and enhanced thermopower are clearly

interrelated. As a direct evidence of a complex structure of doped holes, the recent angular resolved photoemission (ARPES) experiments [5, 11] observed lineshapes that are typical for strongly correlated systems. Paradoxically again, the many-body effects in ARPES are enhanced approaching the band insulator limit [5].

This Letter presents a theory resolving this puzzling situation in layered cobaltates. We show that holes doped into nonmagnetic band insulators  $\text{NaCoO}_2$  and misfits are indeed a composite objects with a broad energy-momentum distribution of their spectral functions. Besides a reduction of the quasiparticle peaks, they display also a dispersive incoherent structure as observed [5, 11]. The underlying physics behind this unexpected complexity is in fact quite simple and based on a unique aspect of  $\text{Co}^{3+}$  ions, i.e., their spin-state quasidegeneracy, and on special lattice geometry of  $\text{CoO}_2$  layers.

In oxides,  $\text{Co}^{2+}$  is always in a high-spin  $3/2$  state while  $\text{Co}^{4+}$  ions usually adopt a low-spin  $1/2$ . Roughly, this selection is decided by the Hund coupling favoring high-spin values, or by the  $t_{2g}$ - $e_g$  crystal field splitting  $10Dq$  supporting low-spin states. An intermediate case is realized for the  $\text{Co}^{3+}$  ions where the  $S = 0, 1, 2$  states strongly compete. This leads to a distinct property  $\text{Co}^{3+}$  rich oxides called “spin-state-transition”, which is responsible for many anomalies such as thermally or doping induced spin-state change in  $\text{LaCoO}_3$  [12, 13], and a spin-blockade effect in  $\text{HoBaCo}_2\text{O}_{5.5}$  [14], to mention a few manifestations of the Janus-like behavior of  $\text{Co}^{3+}$ .

New situation encountered in layered cobaltates – and this is the key point – is that  $\text{CoO}_6$  octahedra are edge-shared. In this geometry, the charge transfer between Co ions occurs along the  $90^\circ$   $d$ - $p$ - $d$  bonds, where the largest matrix element for the hole motion is that between the neighboring orbitals of  $t_{2g}$  and  $e_g$  symmetry (see  $\tilde{t}$  process in Fig. 1). This implies that a doped hole dynamically creates  $S = 1$   $t_{2g}^5 e_g^1$  states of  $\text{Co}^{3+}$  [15]. It is this point where the holes – doped into an initially nonmagnetic background – become many-body objects dressed

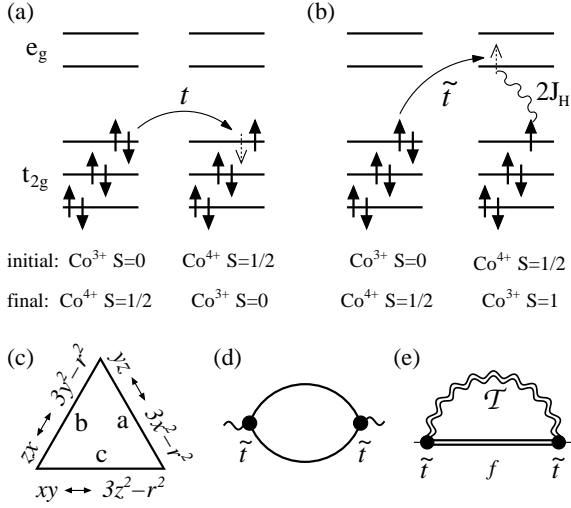


FIG. 1: (a) A conventional  $t$ -hopping within the low-spin  $t_{2g}$  states. (b)  $\tilde{t}$ -hopping process creating an excited  $Co^{3+} S = 1$  state. Because of the Hund coupling  $J_H$ , this triplet state is quasidegenerate to the  $t_{2g}^6 S = 0$  state, i.e. the excitation energy  $E_T \sim 10Dq - 2J_H$  is low. (c) Bond directions  $a$ ,  $b$ ,  $c$  in the triangular lattice of Co ions and  $\tilde{t}$ -coupled orbitals on these bonds. (d) Selfenergy of the  $\mathcal{T}$  spin excitation. (e) Selfenergy of the holes in a selfconsistent Born approximation.

by virtual spin excitations. Formation of spin polarons suppresses the plane-wave like motion of holes. However, they gain in the kinetic energy by exploiting an additional,  $\tilde{t}$  hopping channel.

The layered structure of cobaltates results in quasi two-dimensional electronic states like in cuprates. This should also lower the symmetry of the  $t_{2g}$  bands (threefold-degenerate in the case of a cubic lattice) that accommodate doped holes. Indeed, ARPES data shows a very simple Fermi surface derived from a single band of  $a_{1g}$  symmetry [5, 11]. This band can be described by the nearest-neighbor Hamiltonian  $H_t = -t \sum_{ij\sigma} f_{j\sigma}^\dagger f_{i\sigma}$ , where the fermionic operators  $f$  represent  $a_{1g}$  holes. They are subject to a conventional Gutzwiller constraint (at most one hole at given site) but this is not much relevant at small density of holes, i.e., near the band-insulator limit. Hence, holes move freely as in a semiconductor.

In contrast, the  $t_{2g}-e_g$  hopping in Fig. 1(b) represents the many-body process as it produces the  $Co^{3+} S = 1$  excitation. The model describing this process has been derived in Ref. [16] and reads as follows:

$$H_{\tilde{t}} = -\frac{\tilde{t}}{\sqrt{3}} \sum_{ij} \left[ \mathcal{T}_{+1,\gamma}^\dagger(i) f_{j\downarrow}^\dagger f_{i\uparrow} - \mathcal{T}_{-1,\gamma}^\dagger(i) f_{j\uparrow}^\dagger f_{i\downarrow} - \mathcal{T}_{0,\gamma}^\dagger(i) \frac{1}{\sqrt{2}} (f_{j\uparrow}^\dagger f_{i\uparrow} - f_{j\downarrow}^\dagger f_{i\downarrow}) + \text{h.c.} \right]. \quad (1)$$

Here,  $\mathcal{T}$  is the spin-triplet excitation generated by hopping of an electron from  $Co_j^{3+}$  to the  $e_g$  level of  $Co_i^{4+}$

(described as hole motion). The process, of course, conserves the total spin. In addition, the direction  $\gamma$  of the bond  $\langle ij \rangle$  selects the  $e_g$  orbital involved in  $\tilde{t}$  process [see Fig.1(c)], according to  $E_g$  symmetry relations between  $\mathcal{T}_\gamma$  operators:  $\mathcal{T}_c = \mathcal{T}_{3z^2-r^2}$ ,  $\mathcal{T}_{a/b} = -\frac{1}{2}\mathcal{T}_{3z^2-r^2} \pm \frac{\sqrt{3}}{2}\mathcal{T}_{x^2-y^2}$ .

Based on this model, we develop a theory for the photoemission experiments in cobaltates. It is evident from (1), that by creating and destroying  $\mathcal{T}$  excitations as they propagate, the holes are strongly renormalized and we deal with a spin-polaron problem. This resembles the problem of doped Mott insulators like cuprates, however, the nature of spin excitations is different here because of the nonmagnetic ground state. Instead of magnon-like propagating modes as in cuprates, fluctuations of the very spin value of  $Co^{3+}$  ions are the cause of the spin-polaron physics in cobaltates [17].

For the calculation of the fermionic self-energies, we employ the selfconsistent Born approximation [see Fig. 1(e)], which has extensively been used in the context of spin-polarons in cuprates [21]. First, we focus on spin excitation spectrum. Since a direct  $e_g-e_g$  hopping in case of  $90^\circ$ -bonds is not allowed by symmetry, the bare  $\mathcal{T}$  spin excitation is a purely local mode, at the energy  $E_T$ . The coupling to the holes in (1) shifts and broadens this level. Accounting for this effect perturbatively [see Fig. 1(d)], we obtain the  $\mathcal{T}$  Green's function  $\mathcal{D}^{-1}(i\omega) = i\omega - E_T - \Sigma_T(i\omega)$  with

$$\Sigma_T(i\omega) = \frac{2\tilde{t}^2}{3\beta} \sum_{\mathbf{k}\mathbf{k}',i\epsilon} \Gamma_{\mathbf{k}} \mathcal{G}_0(\mathbf{k}, i\epsilon) \mathcal{G}_0(\mathbf{k}', i\epsilon + i\omega). \quad (2)$$

Here,  $\mathcal{G}_0$  is the bare electron propagator  $\mathcal{G}_0(\mathbf{k}, i\epsilon) = (i\epsilon - \xi_{\mathbf{k}})^{-1}$  with the  $a_{1g}$  dispersion on a triangular lattice  $\xi_{\mathbf{k}} = -2t(c_a + c_b + c_c) + \mu$ , where  $c_\gamma = \cos k_\gamma$  and  $k_\gamma$  are the projections of  $\mathbf{k}$  on  $a, b, c$  directions. The underlying  $E_g$  symmetry of  $\mathcal{T}$  operators involved in  $\tilde{t}$  hopping results in the factor  $\Gamma_{\mathbf{k}} = c_a^2 + c_b^2 + c_c^2 - c_a c_b - c_b c_c - c_c c_a$ . We neglected a weak momentum dependence of  $\Sigma_T$  for the sake of simplicity. This is justified as long as  $\Sigma_T$  is small compared to the spin gap  $E_T$ .

Further, we approximate  $\Gamma_{\mathbf{k}}$  by its Brillouin-zone average  $3/2$ , obtaining the simple expressions for  $\Sigma_T$  in terms of bare fermionic density of states  $N_0(x) = \sum_{\mathbf{k}} \delta(x - \xi_{\mathbf{k}})$ :

$$\text{Im}\Sigma_T(E) = -\pi\tilde{t}^2 \int_{-E}^0 dx N_0(x) N_0(x + E), \quad (3)$$

$$\text{Re}\Sigma_T(E) = -\tilde{t}^2 \int_{-\infty}^0 dx \int_{x^2}^{\infty} dy^2 \frac{N_0(x) N_0(x + y)}{y^2 - E^2}, \quad (4)$$

These equations determine the renormalized spin-excitation spectrum  $\rho_T(E) = -\pi^{-1} \text{Im}\mathcal{D}(i\omega \rightarrow E + i\delta)$  used below for calculation of the fermionic selfenergy.

The selfenergy diagram in Fig. 1(e) reads as:

$$\Sigma_{\mathbf{k}}(i\epsilon) = -\frac{2\tilde{t}^2}{\beta} \sum_{\mathbf{k}', i\omega} [\Gamma_{\mathbf{k}'} \mathcal{D}(-i\omega) + \Gamma_{\mathbf{k}} \mathcal{D}(i\omega)] \mathcal{G}(\mathbf{k}', i\epsilon + i\omega), \quad (5)$$

where  $\mathcal{G}^{-1}(\mathbf{k}, i\epsilon) = i\epsilon - \xi_{\mathbf{k}} - \Sigma_{\mathbf{k}}(i\epsilon)$ . We can write  $\Sigma_{\mathbf{k}}(\omega) = 2\tilde{t}^2 [\Phi(\omega) + \Gamma_{\mathbf{k}} \Xi(\omega)]$ , where

$$\Phi(\omega) = \int_0^\infty dE \rho_T(E) \int_0^\infty dx \frac{\tilde{N}(x)}{\omega - E - x + i\delta}, \quad (6)$$

$$\Xi(\omega) = \int_0^\infty dE \rho_T(E) \int_{-\infty}^0 dx \frac{N(x)}{\omega + E - x + i\delta}. \quad (7)$$

The full local density of states  $N(E) = \sum_{\mathbf{k}} A(\mathbf{k}, E)$  and its  $E_g$  symmetry part  $\tilde{N}(E) = \sum_{\mathbf{k}} \Gamma_{\mathbf{k}} A(\mathbf{k}, E)$  are functions of the selfenergy itself, via the spectral functions  $A(\mathbf{k}, E) = -\pi^{-1} \text{Im} \mathcal{G}(i\epsilon \rightarrow E + i\delta)$ . The above equations are thus to be solved self-consistently.

Next, we would like to test the reliability of approximations made. To this end, we performed an exact diagonalization of our model  $H = H_t + H_{\tilde{t}}$  on a  $\sqrt{7} \times \sqrt{7}$  hexagonal cluster [Fig. 2(d)]. We inject one hole on such a cluster and calculate its spectral function

$$A(\mathbf{k}, E) = -\frac{1}{\pi} \text{Im} \langle GS | f_{\mathbf{k},\sigma}(z - H)^{-1} f_{\mathbf{k},\sigma}^\dagger | GS \rangle, \quad (8)$$

where  $z = E + E_{GS} + i\delta$ . Since the groundstate  $|GS\rangle$  contains no holes and the single hole on the cluster represents 1/7 doping, the effective doping is about 10%. Periodic boundary conditions allow us to access  $A(\mathbf{k}, E)$  at two non-equivalent  $\mathbf{k}$  points [see Fig. 2(d)]. To obtain continuous profiles of  $A(\mathbf{k}, E)$ , we have broadened the excited states.

Our model has two parameters:  $\tilde{t}/t$  and  $E_T/t$ . In fact, the ratio  $\tilde{t}/t \simeq 3$  follows from the relations  $t = 2t_0/3$  and  $\tilde{t}/t_0 = t_\sigma/t_\pi \simeq 2$  (where  $t_0 = t_\pi t_\pi / \Delta_{pd}$ ) [16]. Thus, we set below  $\tilde{t}/t = 3$ , leaving  $E_T$  as a free parameter.

We find that the above equations give results consistent with the exact diagonalization data, even at rather small spin gap values  $E_T \sim t$ , as shown in Fig. 2(a,c). Both approaches lead to spectral functions with a renormalized quasiparticle (qp-) peak whose spectral weight is transferred to a pronounced hump structure. [A peculiar momentum dependence of the matrix elements  $\Gamma_{\mathbf{k}}$  (note that  $\Gamma_{\mathbf{k}=0} = 0$ ) reduces the effect at  $\mathbf{k} = \Gamma$  point]. Several maxima on the hump reflect the presence of multiple triplet excitations created by the hole propagation. All these are the typical signatures of polaron physics. Multiplet structure of the hump will in reality be smeared by phonons which are naturally coupled to the  $\tilde{t}$  transition involving also the orbital sector. Although experiments [22] indicate that electron-phonon coupling is moderate in cobaltates, it may substantially enhance the spin-polaron effects, as in case of cuprates [23].

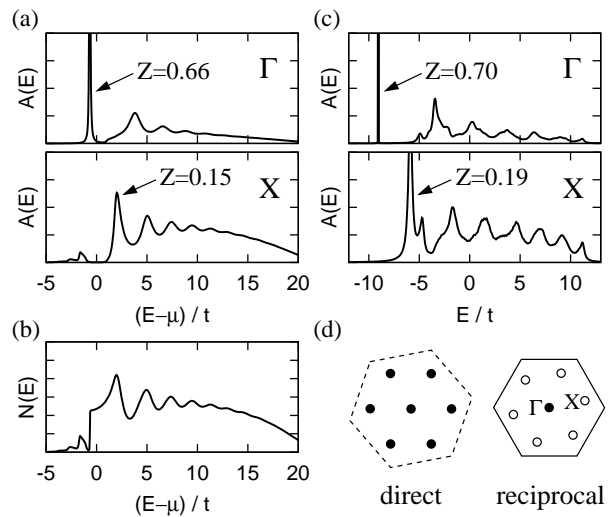


FIG. 2: Comparison of results from the diagrammatic calculation at 10% doping (left) and from exact diagonalization (right). (a) Spectral functions and a quasiparticle weight  $Z$  obtained from Eqs. (3)–(7) with bare  $E_T = 1.2t$  (renormalized to  $\tilde{E}_T/t \approx 1$  by interactions) and (b) the corresponding density of states  $N(E)$ . The incoherent structure dominates  $N(E)$ . A peak around  $2t$  corresponds to the van Hove singularity smeared by interaction effects. (c) Spectral functions from exact diagonalization at  $E_T/t = 1$ . (d) The 7-site cluster in direct space (the dashed line defines the supercell) and in reciprocal space (full line is the Brillouin zone boundary). The allowed  $\mathbf{k} = \Gamma, X$  points are indicated by  $(\bullet)$  and  $(\circ)$ .

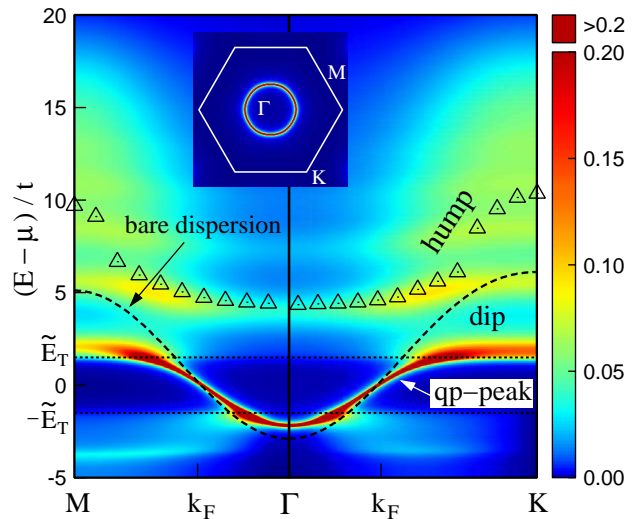


FIG. 3: (Color online) Intensity map of the spectral density  $A(\mathbf{k}, E)$  of the  $\text{Co}^{4+}$  holes along M- $\Gamma$ -K path in the Brillouin zone calculated at 30% doping and  $E_T = 2t$ . As the hole energy reaches the renormalized spin excitation energy  $\tilde{E}_T$ , the qp-peak broadens and its weight is transferred to a broad, incoherent structure. This results in a “peak-dip-hump” profile of  $A(\mathbf{k}, E)$  seen also in Fig. 2. The top of the smoothed hump structure is indicated by triangles. The dashed line shows the bare dispersion. The Fermi surface is shown in the inset.

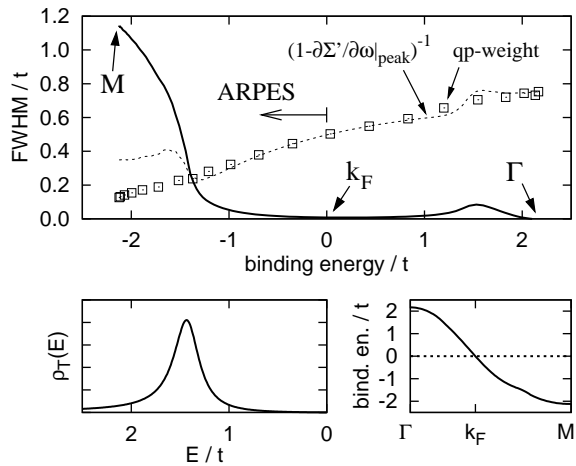


FIG. 4: Top panel: Full energy width at half maximum of the quasiparticle peak along the M- $\Gamma$  dispersion curve (see bottom-right panel) plotted as a function of the binding energy. The part from  $k_F$  to M is accessible by ARPES experiments. Strong qp-damping below  $\sim -1.4t$  is due to a scattering on  $S = 1$  excitations. The spectral weight of the qp-peak obtained by a direct integration is indicated by squares. When damping is small, it coincides with a conventional qp-residue  $(1 - \partial\Sigma'/\partial\omega)^{-1}$ . Lower panel: The  $\mathcal{T}$ -exciton spectral function (left), and renormalized hole dispersion (right).

To illustrate the gross features of the hole renormalization, in Fig. 3 we show a complete map of the spectral function along M- $\Gamma$ -K path in the Brillouin zone. We have used a representative value  $E_T = 2t$  which is renormalized by holes to  $\tilde{E}_T \approx 1.4t$ . Compared to the bare dispersion, the bandwidth of the renormalized holes is reduced by a factor  $\sim 2$ . The main observation here is that as the hole energy reaches  $\tilde{E}_T$ , the dynamical generation of  $S = 1$  excitations becomes very intense and a broad incoherent response develops, leading to the pronounced “peak-dip-hump” structure of  $A(\mathbf{k}, E)$ . Following the maximum of the smoothed hump structure, we observe its strong dispersion (stemming also from incoherent  $\tilde{t}$  hopping).

Fig. 3 suggests a possible determination of  $\tilde{E}_T$  from the quasiparticle damping. To address this problem, in Fig. 4 we show the energy width of the qp-peak following its dispersion curve. The sharp onset of the damping at the binding energy  $\approx -1.4t$  is clearly related to the maximum of the spin-excitation spectral function  $\rho_T(E)$ . In addition, Fig. 4 shows the weight of the qp-peak which is  $\mathbf{k}$ -dependent (mainly due to the matrix element  $\Gamma_{\mathbf{k}}$ ).

Comparison of Figs. 3 and 4 with the data of Refs. 5, 11 reveals a remarkable correspondence between theory and experiment. In particular, both the qp-peak and the hump dispersions (see Figs. 2 and 3 of Ref. 5) are well reproduced by theory, considering  $t \approx 100\text{meV}$  suggested by the band structure fit [24]. The onset energy  $\tilde{E}_T \sim$

$1.4t$  for the qp-damping (Fig. 4) is then  $\approx 140\text{meV}$ , in nice agreement with experiment (see Fig. 2c of Ref. 5). Physically, dilute spin-polarons are expected to be pinned by disorder, thus qp-peaks should be suppressed at low hole doping.

To summarize, we have presented a theory for the photoemission experiments in layered cobaltates. A strong damping of quasiparticles, their reduced spectral weights, broad and dispersive incoherent structures, and a “peak-dip-hump” type lineshapes all find a coherent explanation within our model. We thus conclude that unusual correlations observed near the band insulator regime of cobaltates are the direct manifestation of the spin-state quasidegeneracy of Co ions, and this intrinsic feature of cobaltates should be the key for understanding of their unique physical properties, such as the high thermopower. In particular, the spin-polaronic nature of charge carriers should be essential for explanation of its remarkable magnetic field sensitivity [2].

We would like to thank B. Keimer for stimulating discussions. This work was partially supported by the Ministry of Education of CR (MSM0021622410).

- 
- [1] N.F. Mott, *Metal-Insulator Transitions*, (Taylor and Francis, London, 1974).
  - [2] Y. Wang, N.S. Rogado, R.J. Cava, and N.P. Ong, *Nature (London)* **423**, 425 (2003).
  - [3] M.L. Foo *et al.*, *Phys. Rev. Lett.* **92**, 247001 (2004).
  - [4] J. Bobroff *et al.*, *cond-mat/0704.3512*.
  - [5] V. Brouet *et al.*, *cond-mat/0706.3849*.
  - [6] G. Lang *et al.*, *Phys. Rev. B* **72**, 094404 (2005).
  - [7] C. de Vaulx *et al.*, *Phys. Rev. Lett.* **95**, 186405 (2005).
  - [8] S.P. Bayrakci *et al.*, *Phys. Rev. Lett* **94**, 157205 (2005).
  - [9] C. de Vaulx *et al.*, *Phys. Rev. Lett.* **98**, 246402 (2007).
  - [10] M. Lee *et al.*, *Nature Materials* **5**, 537 (2006).
  - [11] D. Qian *et al.*, *Phys. Rev. Lett.* **97**, 186405 (2006).
  - [12] M.W. Haverkort *et al.*, *Phys. Rev. Lett.* **97**, 176405 (2006).
  - [13] S. Yamaguchi, Y. Okimoto, H. Taniguchi, and Y. Tokura, *Phys. Rev. B* **53**, R2926 (1996).
  - [14] A. Maignan *et al.*, *Phys. Rev. Lett.* **93**, 026401 (2004).
  - [15]  $t_{2g}^4 e_g^2$ ,  $S = 2$  configuration is not accessible by hopping.
  - [16] G. Khaliullin and J. Chaloupka, *cond-mat/0707.2364*.
  - [17] In contrast to Refs. [18, 19], where a *static* hole surrounded by  $S = 1$   $\text{Co}^{3+}$  ions was studied, in the present model the triplet  $S = 1$  excitations are *virtual* and generated dynamically by the *very motion* of the hole via the  $\tilde{t}$  process. These two pictures can merge if a hole is strongly trapped (*e.g.*, by Na-potential [20]).
  - [18] G. Khaliullin, *Prog. Theor. Phys. Suppl.* **160**, 155 (2005).
  - [19] M. Daghofer, P. Horsch, and G. Khaliullin, *Phys. Rev. Lett.* **96**, 216404 (2006).
  - [20] M. Roger *et al.*, *Nature (London)* **445**, 631 (2007).
  - [21] See, *e.g.*, C.L. Kane, P.A. Lee, and N. Read, *Phys. Rev. B* **39**, 6880 (1989).
  - [22] J.-P. Rueff *et al.*, *Phys. Rev. B* **74**, 020504(R) (2006).
  - [23] A.S. Mishchenko and N. Nagaosa, *Phys. Rev. Lett.* **93**,

036402 (2004); O. Rösch and O. Gunnarsson, Phys. Rev. Lett. **93**, 237001 (2004). [24] S. Zhou *et al.*, Phys. Rev. Lett. **94**, 206401 (2005).